PHYSICAL REVIEW D **73,** 124035 (2006)

Superradiant instability of large radius doubly spinning black rings

Óscar J. C. Dias*

Perimeter Institute for Theoretical Physics, Waterloo, Ontario N2L 2Y5, Canada
and Department of Physics, University of Waterloo, Waterloo, Ontario N2L 3G1, Canada
(Received 13 February 2006; published 23 June 2006)

We point out that 5D large radius doubly spinning black rings with rotation along S^1 and S^2 are afflicted by a robust instability. It is triggered by superradiant bound state modes. The Kaluza-Klein momentum of the mode along the ring is responsible for the bound state. This is shown by analyzing the boosted Kerr black string. The present kind of instability in black strings and branes was first suggested by Marolf and Palmer and studied in detail by Cardoso, Lemos and Yoshida. We find the frequency spectrum and time scale of this instability in the black ring background, and show that it is active for infinite-radius rings with large rotation along S^2. We identify the end point of the instability and argue that it provides a dynamical mechanism that introduces an upper bound in the rotation of the black ring. To estimate the upper bound, we use the recent black ring model of Hovdebo and Myers, with a minor extension to accommodate an extra small angular momentum. This dynamical bound can be smaller than the Kerr-like bound imposed by regularity at the horizon. Recently, the existence of higher-dimensional black rings has been conjectured. They will be stable against this mechanism.

DOI: 10.1103/PhysRevD.73.124035 PACS numbers: 04.50.+h, 04.20.Jb, 04.30.Nk, 04.70.Bw

I. INTRODUCTION

It is not an easy problem to find exact black hole solutions with a clear physical interpretation in gravity theories, but it is not less difficult to prove or discard their uniqueness and stability. In four dimensions, years of research ended with the conclusion that the Kerr black hole solution is stable and satisfies a uniqueness theorem.

The higher-dimensional arena, both in the vacuum Einstein theory and in its extension to include the supergravity fields of low energy string theory, has a broad variety of black hole solutions. For example, five-dimensional (5D) Einstein theory allows not only the existence of black holes with topology S^3—the Tangherlini black hole [1] and the Myers-Perry black hole [2]—but also the Emparan-Reall black ring with topology $S^1 \times S^2$ [3], and extended objects known as black strings [4].

This higher variety of solutions suggests that the uniqueness theorem might not be valid in higher dimensions. The uniqueness of the 5D Myers-Perry solution for black holes with topology S^3, and with two commuting spacelike Killing vectors and a stationary timelike Killing vector, has been proven [5]. However, when other topologies and Killing symmetries are considered, the uniqueness theorem is violated as the discovery of the black ring explicitly proves. In five dimensions, a black hole can rotate along two distinct planes. The rotating black ring of [3] has angular momentum only along S^1. Setting one of the angular momenta equal to zero in the Myers-Perry black hole, there is an upper bound for the ratio between the angular momentum J and the mass M of the black hole, $J^2/M^3 \leq 32/(27\pi)$, while for the black ring there is a lower bound in the above ratio, $J^2/M^3 \geq 1/\pi$, i.e., there is a minimum rotation that is required in order to prevent the black ring from collapsing. Now, what is quite remarkable is that for $1/\pi \leq J^2/M^3 \leq 32/(27\pi)$ there are Myers-Perry black holes and Emparan-Reall black rings with the same values of M and J. Moreover, for the same values of the conserved charges, there are actually two branches of black rings differing in the size of their radius. The uniqueness in higher dimensions is further violated when extra conserved charges and dipole charges are included [6–9]. For our purposes, it will be important to note that one of the parameters that characterizes the Emparan-Reall black ring is its radius, R [3]. When this radius goes to zero the black ring reduces to the Myers-Perry black hole, while in the infinite-radius limit it yields a boosted black string. Recently, a vacuum black ring solution with angular momentum along S^2 (but no rotation along S^1) was found by Mishima and Iguchi [10]. This solution was rediscovered and properly interpreted by Figueras [11]. Since this solution does not rotate along S^1, it is balanced by the pressure of a conical disk. When its radius goes to zero the black ring reduces to the Myers-Perry black hole, while in the infinite-radius limit it yields a Kerr black string [11]. The most general element of the vacuum black ring family of solutions—hereafter dubbed doubly spinning black ring—with rotation along both S^1 and S^2 is still not yet known. However, we know that it will reduce to [3] or [11] when one of the rotations vanishes. Moreover, the zero-radius limit of this doubly spinning black ring will be a 5D Myers-Perry black hole with two angular momenta, and the infinite-radius limit will yield a boosted Kerr black string.

Black hole solutions in higher dimensions also bring new challenges to the stability issue. Some progress is being slowly achieved. The stability of Tangherlini black

*Also at KITP–Kavli Institute for Theoretical Physics, UCSB, Santa Barbara, CA 93106, USA.
Electronic address: odias@perimeterinstitute.ca

holes is established [12]. However, in the higher-dimensional arena it has been progressively realized that instability is more the rule rather than the exception. There are indeed several instabilities that afflict higher-dimensional objects, and some of them can be grouped in the following classes.

(a) The Gregory-Laflamme instability [13]: This gravitational instability is active in extended black objects like black strings, black branes, and at least large radius black rings [14,15]. The unstable modes are long wavelength modes along the string, so this instability can be eliminated by reducing the radius of the compactification along the string. For a fixed radius, it is also suppressed by boosting the solution along the string direction [15].

(b) Superradiant instability: Superradiant scattering, where an incident wave packet can be reflected with a stronger amplitude, can lead to an instability if, e.g., we have a reflecting wall surrounding the black hole that scatters the returning wave back toward the horizon. In such a situation, the wave will bounce back and forth, between the mirror and the black hole, amplifying itself each time. The total extracted energy grows exponentially until finally the radiation pressure destroys the mirror. This is Press and Teukolsky's black hole bomb, first proposed in [16] and studied in detail in [17]. This instability can arise with a natural ''mirror'' in a variety of situations: a massive scalar field in a Kerr background creates a potential that can cause flux to scatter back toward the horizon [18]; infinity in asymptotically anti-de Sitter (AdS) spaces also provides a natural wall that leads, for certain conditions, to an instability [19]; a wave propagating around spinning black strings may similarly find itself trapped, because the Kaluza-Klein (KK) momentum along the string can provide a potential barrier at infinity [20–22]. The unstable modes can be scalar, electromagnetic or gravitational. In general, but with exceptions, this instability can be present for arbitrary values of angular momentum of the geometry.

(c) Gyration instability: In the context of D1-D5-P black strings, it was found that a spinning black string, whose angular momentum exceeds a certain critical value, decays into a gyrating black string in which part of the original angular momentum is carried by gyrations of the string [20]. The gyrating string has a helical profile traveling along the string with the velocity of light. This instability is active for long strings with large angular momentum.

(d) Ultraspin instability: In six or higher spacetime dimensions, there is no upper bound for the rotation of the Myers-Perry black hole [2]. However, it was argued [23] that a Gregory-Laflamme-like instability will arise to dynamically enforce a Kerr-like bound in these cases. While this analysis does not directly apply in five dimensions, entropy arguments suggest an analogous instability still exists and will lead to the formation of a black ring if the angular momentum is too large [3].

(e) Ergoregion instability: Geometries that have an ergoregion but are horizon-free develop this kind of instability [24]. It occurs in rotating stars with an ergoregion [25], as well as in smooth nonsupersymmetric D1-D5-P geometries [26].

In this paper we point out that 5D doubly spinning back rings can be expected to suffer from the superradiant instability described in item (b), and we find its properties. This instability is triggered by two factors that occur simultaneously. On one hand, the KK momentum of the waves along the ring works effectively as a massive term that provides a potential barrier at infinity. This potential barrier allows the appearance of a potential well where bound states get trapped. On the other hand, the bound state modes can suffer superradiant amplification in the ergoregion. The unstable modes are then waves that bounce back and forth between the ergoregion and the potential barrier, and that are amplified in each scattering. This kind of instability, where the bound states are induced by the KK momentum, was first suggested by Marolf and Palmer [20], and explicitly studied by Cardoso, Lemos and Yoshida [21,22]. This is the same instability, but with a different source for the bound states, as the one studied in [16–19].

To fully study analytically this instability in the black ring geometry we would have to separate the wave equation in this background. However, it is not possible to do this separation even in the scalar case or even in the black ring with rotation only along S^1. This is explicitly shown in [27], where the term that impedes this wave separation is identified. This obstacle is closely connected with the fact that the Hamiltonian-Jacobi equation for the geodesics is also not separable [28], and ultimately with the fact that the solution does not have a Killing tensor [29]. An investigation of waves in this geometry will have to be done using full 3D numerical simulations. Given this handicap (and the fact that the finite radius doubly spinning black ring metric is still not yet known), we do what can be done analytically: we consider the large radius limit of the doubly spinning black ring—which yields a boosted Kerr black string—and we verify that this instability is active in this background. We then compactify the string direction to find conclusions about the instability in finite radius black rings.

Whenever one has an instability, we naturally ask what its end point is. Usually, it is remarkably difficult to give a definite answer to this question. For example, the ultimate fate of the Gregory-Laflamme instability [30,31], the gyration instability [20], and the ergoregion instability [26] still remains an open issue. However, the superradiant instabilities are special, in the sense that we usually can make strong statements about their end point. This follows

from the fact that the growth of this type of instability is fed by the rotational energy of the background geometry which decreases during the process. In our case, we will conclude that the boosted Kerr black string will release all its angular momentum, and will settle down into a nonrotating boosted black string. However, as a consequence of the KK momentum quantization that occurs when we compactify a black string, we will argue that finite radius black rings will not lose all their angular momentum along S^2. Therefore, in practice this means that the superradiant instability provides a dynamical mechanism that imposes an upper bound for the rotation of the black rings along S^2. Note that, due to the presence of other instabilities on the system, like, e.g., the Gregory-Laflamme one, we expect that a classical evolution of the black ring will proceed with the contribution of all the instabilities that afflict the system. It is not clear yet what the exact end state of this evolution is.

The plan of this paper is organized as follows. In Secs. II, III, and IV it is argued that 5D doubly spinning black rings are expected to be unstable. In Sec. II we review the relevant black ring geometries and their large radius limit. In Sec. III we separate the Klein-Gordon equation in the infinite-radius black ring background, and we discuss the relevant ingredients and properties of the instability. The quantitative features of the instability, namely, its frequency spectrum and its time scale, are computed in Sec. IV, using the matched asymptotic method. The stability analysis of the higher-dimensional boosted Myers-Perry black string is carried out in Sec. V, where it is shown that they are stable against the superradiant mechanism. The eventual implications of this result to the stability of higher-dimensional rings is then discussed. Finally, in Sec. VI we discuss the results, with an emphasis given to the issue of the instability end point. In particular, we argue that the instability discussed in this paper provides a mechanism that effectively bounds the rotation of doubly spinning black rings. We estimate the upper bound, both on the rotation along S^1 and S^2, using the recent black ring model of [15], with a minor extension to accommodate an extra small angular momentum.

II. BLACK RING GEOMETRIES AND THEIR LARGE RADIUS LIMIT

A. The black ring with rotation along S^1

The first element of the family of 5D black rings was found by Emparan and Reall [3] and is described by (here we write the metric in the form displayed in [7] after using the factorization of [32])

$$ds^2 = -\frac{F(y)}{F(x)}\left(dt + R\sqrt{\lambda(\lambda-\nu)}\frac{1+\lambda}{1-\lambda}\frac{1+y}{F(y)}d\psi\right)^2 + \frac{R^2}{(x-y)^2} \times F(x)\left[-\frac{G(y)}{F(y)}d\psi^2 - \frac{dy^2}{G(y)} + \frac{dx^2}{G(x)} + \frac{G(x)}{F(x)}d\phi^2\right], \quad (1)$$

where

$$F(\xi) = 1 + \lambda\xi, \qquad G(\xi) = (1-\xi^2)(1+\nu\xi). \quad (2)$$

The coordinates x and y vary within the ranges

$$-1 \le x \le 1, \qquad -\infty < y \le -1. \quad (3)$$

To avoid conical singularities the period of the angular coordinates ϕ and ψ must be

$$\Delta\phi = \Delta\psi = \frac{2\pi\sqrt{1-\lambda}}{1-\nu}, \quad (4)$$

and the parameters λ and ν must satisfy the relation

$$\lambda = \frac{2\nu}{1+\nu^2}, \qquad 0 < \nu < 1. \quad (5)$$

This condition guarantees that the rotation of the ring balances the gravitational self-attraction of the ring.

The black ring has a curvature singularity at $y = -\infty$. The regular event horizon of topology $S^1 \times S^2$ is at $y = -1/\nu$. The ergosphere is located at $y = -1/\lambda$. The solution is asymptotically flat with the spatial infinity being located at $x = -1$ and $y = -1$. When $\lambda = \nu$ the geometry (1) describes a static black ring without rotation, whose dynamical equilibrium is ensured by a conical singular disk whose pressure balances the self-gravitational attraction of the ring.

We will be particularly interested in the large radius limit of (1), which is defined by taking [7]

$$R \to \infty, \qquad \lambda \to 0, \quad \text{and} \quad \nu \to 0, \quad (6)$$

in the solution (1), and keeping $R\nu$ and λ/ν finite. More particularly, take

$$R\nu = 2M, \qquad \frac{\lambda}{\nu} = \cosh^2\sigma, \qquad r = -\frac{R}{y}, \qquad \cos\theta = x, \qquad z = R\psi, \quad (7)$$

where M and σ are constants. Then the black ring solution (1) goes over to the boosted black string solution with horizon located at $r = 2M$ and with boost angle $\tanh\sigma = 1/\sqrt{2}$. This particular value of the boost angle is the one that follows from the balance condition (5). This solution can also be constructed by applying a Lorentz boost with angle σ to the geometry four-dimensional (4D) Schwarzschild $\times \mathbb{R}$ [6]. The parameter M is the mass density of the black string extended along the z direction.

The black ring solution can be extended in order to include electric charge [6,7], as well as magnetic dipole charge [8]. The most general known seven-parameter family of nonsupersymmetric black ring solutions, that includes the above solutions as special cases, was presented in [9]. It is characterized by three conserved charges, three dipole charges, two unequal angular momenta, and a parameter that measures the deviation from the supersymmetric configuration. In the black ring background, the Penrose process was discussed in [33], perturbation analysis in the large radius limit was carried out in [27], and an ultrarelativistic boost of the black ring was

considered in [34]. The algebraic classification of the black ring is done in [35]. There are also supersymmetric black rings that we will not discuss in this paper. A recent detailed discussion of the supersymmetric black ring system can be found, e.g., in [36].

B. The black ring with rotation along S^2

The 5D rotating black ring with rotation along S^2 (and no rotation along S^1) was found by Mishima and Iguchi [10] and Figueras [11]. In its most appropriate form for physical interpretation [11], the line element is

$$\begin{aligned} ds^2 = &-\frac{H(\lambda,y,x)}{H(\lambda,x,y)}\left(dt-\frac{\lambda a y(1-x^2)}{H(\lambda,y,x)}d\phi\right)^2 \\ &+\frac{R^2 H(\lambda,x,y)}{(x-y)^2}\Bigg[-\frac{dy^2}{(1-y^2)F(\lambda,y)} \\ &-\frac{(1-y^2)F(\lambda,x)}{H(\lambda,x,y)}d\psi^2+\frac{dx^2}{(1-x^2)F(\lambda,x)} \\ &+\frac{(1-x^2)F(\lambda,y)}{H(\lambda,y,x)}d\phi^2\Bigg], \end{aligned} \tag{8}$$

where

$$\begin{aligned} F(\lambda,\xi) &= 1+\lambda\xi+\left(\frac{a\xi}{R}\right)^2, \\ H(\lambda,\xi_1,\xi_2) &= 1+\lambda\xi_1+\left(\frac{a\xi_1\xi_2}{R}\right)^2. \end{aligned} \tag{9}$$

The coordinates x and y vary in the intervals defined in (3). To avoid conical singularities at $x=-1$ and $y=-1$, the period of the angular coordinates ϕ and ψ must be given by

$$\Delta\phi=\Delta\psi=\frac{2\pi}{\sqrt{1-\lambda+a^2/R^2}}. \tag{10}$$

However, the solution has a conical singularity at $x=1$ that signals the presence of a conical singular disk that balances the self-gravitational attraction of the ring. The parameters λ and a must satisfy the relation

$$\frac{2a}{R}<\lambda<1+\frac{a^2}{R^2}, \tag{11}$$

where the lower bound guarantees that there is a horizon and the upper bound ensures the absence of closed timelike curves. This black ring has a curvature singularity, and a regular event horizon with topology $S^1\times S^2$. It is asymptotically flat with the spatial infinity being located at $x=-1$ and $y=-1$. Moreover, the black ring has rotation along the azimuthal direction ϕ of the S^2, and it also has an ergoregion.

Again, we will be interested in the large radius limit of (8), which is defined by taking [7]

$$R\to\infty \quad \text{and} \quad \lambda\to 0, \tag{12}$$

in the solution (8), and keeping $R\lambda$ fixed. More concretely, take

$$R\lambda=2M, \qquad r=-\frac{R}{y}, \qquad \cos\theta=x, \qquad z=R\psi, \tag{13}$$

where M is a constant. Then the black ring solution (8) goes over to the Kerr black string solution extended along the z direction, with mass density M and rotation parameter a along the azimuthal ϕ direction. This solution can also be constructed by adding a flat direction to the 4D Kerr black hole, yielding 4D Kerr $\times\,\mathbb{R}$.

C. The large radius doubly spinning black ring: Boosted spinning black string

The most general 5D black ring solution—the doubly spinning black ring—is not yet known. This more general element of the family will have rotation both along the plane of the ring (i.e., along the S^1 direction parametrized by ψ) that will balance the self-gravitation of the ring, and along the azimuthal ϕ direction of the S^2. Therefore, when the rotation along S^2 vanishes this doubly spinning solution reduces to (1), while when it is the rotation along S^1 that is absent it reduces to (8).

Although we still do not know the line element of the doubly spinning black ring, we do know the geometry that describes its large radius limit. Indeed, it is not difficult to convince ourselves (see Fig. 1) that in this limit it will be described by a boosted Kerr black string extended along the z direction. This black string is characterized by the mass density M, by the boost angle $\sigma=\operatorname{arctanh}(1/\sqrt{2})$, and by the rotation parameter a along the azimuthal ϕ direction. This can also be constructed by adding a flat direction z to the 4D Kerr black hole, and then applying a Lorentz boost to it, $dt\to\cosh\sigma dt+\sinh\sigma dz$ and $dz\to\sinh\sigma dt+\cosh\sigma dz$. This yields the boosted Kerr black string geometry

$$\begin{aligned} ds^2 = &-\left(1-\frac{2Mr\cosh^2\sigma}{\Sigma}\right)dt^2+\frac{2Mr\sinh(2\sigma)}{\Sigma}dtdz \\ &+\left(1+\frac{2Mr\sinh^2\sigma}{\Sigma}\right)dz^2+\frac{\Sigma}{\Delta}dr^2+\Sigma d\theta^2 \\ &+\frac{(r^2+a^2)^2-\Delta a^2\sin^2\theta}{\Sigma}\sin^2\theta d\phi^2 \\ &-\frac{4Mr\cosh\sigma}{\Sigma}a\sin^2\theta dtd\phi \\ &-\frac{4Mr\sinh\sigma}{\Sigma-2Mr}a\sin^2\theta dzd\phi, \end{aligned} \tag{14}$$

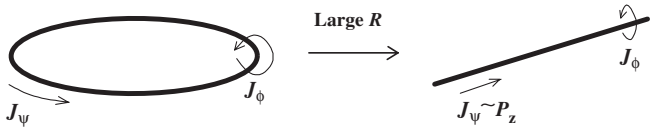

FIG. 1. In the large radius limit, the doubly spinning black ring yields a boosted Kerr black string.

where

$$\Delta = r^2 + a^2 - 2Mr, \qquad \Sigma = r^2 + a^2\cos^2\theta. \tag{15}$$

When we set $a = 0$ and $\sigma = \text{arctanh}(1/\sqrt{2})$, we get a boosted black string that describes a large radius skinny balanced black ring that is also found by taking the limit (6) and (7) in (1). Unbalanced rings give boosted black strings with a general σ. In the data examples that we will give in this paper, we will fix σ to have the balanced value. On the other side, if we set $\sigma = 0$ we get a Kerr black string that describes a large radius skinny black ring that is also obtained by taking the limit (12) and (13) in (8).

The boosted Kerr black string has a curvature singularity at $r = 0$, a Cauchy horizon r_- and an event horizon r_+ at $r_\pm = M \pm \sqrt{M^2 - a^2}$, and an ergosurface at $r_e = M\cosh^2\sigma + \sqrt{M^2\cosh^4\sigma - a^2\cos^2\theta}$. To avoid naked singularities, the rotation is constrained to be $a \leq M$.

Three important parameters of the boosted Kerr black string are the angular velocity of the horizon along the ϕ coordinate, $\Omega_\phi = -(g_{t\phi}/g_{\phi\phi})|_{r=r_+}$, the area per unit length of the horizon, A_H, and the temperature of its horizon, T_H, given by

$$\Omega_\phi = \frac{a\cosh\sigma}{r_+^2 + a^2}, \qquad A_H = 4\pi(r_+^2 + a^2)\cosh\sigma, \qquad T_H = \frac{r_+ - r_-}{4\pi(r_+^2 + a^2)\cosh\sigma}. \tag{16}$$

For completeness note that the linear velocity of the horizon along the string direction, $V_z = -(g_{tz}/g_{zz})|_{r=r_+}$, is given by $V_z = -\tanh\sigma$.

III. THE WAVE EQUATION OF THE BOOSTED KERR BLACK STRING: PROPERTIES OF THE INSTABILITY

In this section we will show that a boosted Kerr black string is unstable, against massless field perturbations, due to the combined effect of the superradiant mechanism and of the presence of an effective reflective wall sourced by the KK momentum of the mode along the string direction. This wall provides the arena for the existence of bound states. The mechanism at play in this instability was recently described in [17,19–22,37]), and is active in *some* extended rotating black objects. The massless scalar field acquires an effective mass (due to the KK momentum in the extra dimension) and this makes the wave bounce back and forth. In each scattering the wave suffers superradiant amplification in the ergosphere and this leads to an instability [20,21]. This superradiant instability will also be present in the case of electromagnetic and gravitational waves.

We extend the analysis carried out in [21,22] for Kerr black strings to the boosted case, and then we further extend this analysis to the black ring case. Generically, the results for boosted black strings are in a way the same as the "boosted results" of unboosted black strings. However, we must be cautious since some exceptions to this rule are already known. For example, a boosted black string has an ergoregion and the Penrose process can occur in this region, while in the unboosted case this phenomena is not present [33]. As another example, it was recently shown [15] that Sorkin's critical dimension [31]—below which stable black strings and small black holes on a compact circle can coexist—is boost dependent and actually vanishes for large boosts. Therefore, the boosted results do not seem to follow trivially from the unboosted ones. As explained in [15], this is intimately connected with the different boundary conditions in the two systems.

A. Separation of the wave equation

The evolution of a scalar field Φ in the background of (14) is governed by the curved space Klein-Gordon equation, $\nabla_\mu\nabla^\mu\Phi = 0$. It is appropriate to use the separation ansatz

$$\Phi = e^{-i\omega t}e^{im\phi}e^{-i\kappa z}S_l^m(\theta)\Psi(r), \tag{17}$$

where $S_l^m(\theta)$ are spheroidal angular functions, and the azimuthal number m takes on integer (positive or negative) values. For our purposes, it is enough to consider positive ω's in (17). Inserting this ansatz into the Klein-Gordon equation, we get the following angular and radial wave equations for $S_l^m(\theta)$ and $\Psi(r)$,

$$\frac{1}{\sin\theta}\partial_\theta(\sin\theta\partial_\theta S_l^m) + \left[a^2(\omega^2 - \kappa^2)\cos^2\theta - \frac{m^2}{\sin^2\theta} + \lambda_{lm}\right]S_l^m = 0, \tag{18}$$

$$\begin{aligned}\Delta\partial_r(\Delta\partial_r\Psi) - \Delta[\kappa^2 r^2 + a^2\omega^2 - 2\omega ma\cosh\sigma + \lambda_{lm}]\Psi \\ + [[\omega(r^2 + a^2) - ma\cosh\sigma]^2 \\ + 2Mr(r^2 + a^2)\cosh^2\sigma[\omega - \kappa\tanh\sigma]^2 - 2Mr(r^2 + a^2)\omega^2 \\ - m^2a^2\sinh^2\sigma + 4\kappa maMr\sinh\sigma]\Psi = 0,\end{aligned} \tag{19}$$

where λ_{lm} is the separation constant that allows the splitting of the wave equation, and is found as an eigenvalue of (18). For small $a^2(\omega^2 - \kappa^2)$, the regime we shall be interested in, the eigenvalues associated with the spheroidal wave functions S_l^m are [38]

$$\lambda_{lm} = l(l+1) + \mathcal{O}(a^2(\omega^2 - \kappa^2)) \approx l(l+1), \tag{20}$$

where the integer l is constrained to be $l \geq |m|$.

B. Boundary conditions: Necessary conditions for the instability.

Together with the wave equation, we must also specify the appropriate boundary conditions for the instability problem. The features of these boundary conditions reveal the two ingredients responsible for the presence of the

instability. We are interested in wave perturbations that develop in the vicinity of the horizon and that propagate both into the horizon and out to infinity. Our boundary conditions therefore require only ingoing flux at the horizon and only outgoing waves at infinity.

At the horizon, the second set of terms proportional to Δ in (19) can be neglected and the radial wave equation reduces to

$$\Delta\partial_r(\Delta\partial_r\Psi) + (r_+^2 + a^2)^2\cosh^2\sigma\left(\omega - \kappa\tanh\sigma - \frac{ma}{(r_+^2 + a^2)\cosh\sigma}\right)^2\Psi = 0, \quad \text{as } r \to r_+, \tag{21}$$

where we made use of $\Delta(r_+) = 0$ which implies $2Mr_+ = (r_+^2 + a^2)$. At infinity, the radial wave equation (19) is dominated by

$$\partial_r(r^2\partial_r\Psi) + (\omega^2 - \kappa^2)r^2\Psi = 0, \quad \text{as } r \to \infty, \tag{22}$$

where we used $\Delta \sim r^2$ as $r \to \infty$. Here, or in (19), we realize that the KK momentum κ contributes effectively as a mass term, $-\kappa^2 r^2$, in the wave equation.

The solutions of these two equations that satisfy our boundary conditions are

$$\Psi(r) \sim \begin{cases} (r - r_+)^{-i\varpi} = e^{-i\varpi\ln(r-r_+)}, & \text{as } r \to r_+, \\ r^{-1}e^{+i\sqrt{\omega^2-\kappa^2}r}, & \text{as } r \to \infty, \end{cases} \tag{23}$$

where we have defined

$$\varpi \equiv \frac{(r_+^2 + a^2)\cosh\sigma}{r_+ - r_-}\left(\omega - \kappa\tanh\sigma - \frac{ma}{(r_+^2 + a^2)\cosh\sigma}\right) \equiv \frac{1}{4\pi T_H}(\omega - \omega_{\text{sup}}), \tag{24}$$

with

$$\omega_{\text{sup}} = \kappa\tanh\sigma + \frac{m\Omega_\phi}{\cosh^2\sigma}, \tag{25}$$

and T_H and Ω_ϕ are, respectively, the temperature and the angular velocity of the horizon of the boosted Kerr black string defined in (16).

The features of the boundary conditions (23) reveal the two ingredients responsible for the presence of the instability. Indeed, at infinity we identify the presence of the KK term or mass term, κ^2, that is responsible for the effective reflective wall. On the other side, at the horizon one identifies the presence of the so-called superradiant factor ϖ. When the frequency of the wave is such that ϖ is negative,

$$\omega < \omega_{\text{sup}}, \tag{26}$$

one is in the superradiant regime, and the amplitude of a (corotating) wave is amplified after each scattering.

It is important to understand why it is $\Psi \sim e^{-i\varpi\ln(r-r_+)}$ and not $\Psi \sim e^{+i\varpi\ln(r-r_+)}$ that always describes an ingoing wave at the horizon, since this is the key source of superradiance. It follows from (17) and (23) that at the horizon the wave solution behaves as $\Phi(t, r)|_{r\to r_+} \sim e^{-i\omega t}e^{-i\varpi\ln(r-r_+)}$. The phase velocity of the wave is then $v_{\text{ph}} \propto -\frac{\omega}{\varpi}$. Now, the value of this phase velocity can be positive or negative depending on the value of ω (when we fix the other parameters), so one might question if the first line of (23) really *always* describes an ingoing wave. As in other applications, what is relevant to find the *physical* ingoing wave solution at the horizon is the group velocity of the wave rather than its phase velocity. The normalized group velocity, v_{gr}, at the horizon is $v_{\text{gr}} = 4\pi T_H\frac{d(-\varpi)}{d\omega} = -1$. This is a negative value that signals that the horizon wave solution in (23) always represents an ingoing wave *independently* of the value of ω, and is thus the correct physical boundary condition. However, note that in the superradiant regime (26), the phase velocity is positive and so waves appear as outgoing to an inertial observer at spatial infinity—energy is in fact being extracted.

Notice that (since we are working with positive ω) superradiance will occur only for positive m, i.e., for waves that are corotating with the black hole. Indeed, the wave function is given by $\Phi(t, \phi) \sim e^{i\omega t + im\phi}$. The phase velocity along the angle ϕ is then $v_\phi = \omega/m$, which for $\omega > 0$ and $m > 0$ is positive, i.e., is in the same sense as the angular velocity Ω_ϕ of the black string.

C. The radial wave equation as a Schrödinger equation: Necessary and sufficient conditions for the instability.

The necessary conditions—superradiant regime and presence of the KK effective mass term—are not, in general, sufficient to guarantee that a instability develops in the geometry as we shall conclude in Sec. V. Necessary and sufficient conditions are that the superradiant regime is active and that *bound states* are present. The requirement of these conditions is better understood by rewriting the radial wave equation (19) in the Schrödinger-like form,

$$\partial_{r_*}^2\chi - V\chi = 0, \quad \text{with} \quad V = -\gamma(\omega - V_+)(\omega - V_-), \quad \Psi = (r_+^2 + a^2)^{-1/2}\chi, \tag{27}$$

and r_* is the usual tortoise coordinate r_*. The explicit form of $\gamma > 0$ and $V_\pm$ will be given in great detail in (65), where we will also consider the higher-dimensional case. At the moment, we are interested in a plot of the behavior of the potentials $V_\pm$. The asymptotic behavior of $V_\pm$ is

$$\lim_{r\to r_+} V_\pm = \omega_{\text{sup}}, \qquad \lim_{r\to\infty} V_\pm = \pm|\kappa|. \tag{28}$$

There are only two distinct cases that we sketch in Fig. 2(a) (unstable case) and in Fig. 2(b) (stable case). In these figures, when ω is above V_+ or below V_- (allowed regions), the solutions have an oscillatory behavior. In those intervals where ω is in between the curves of V_+ and V_-

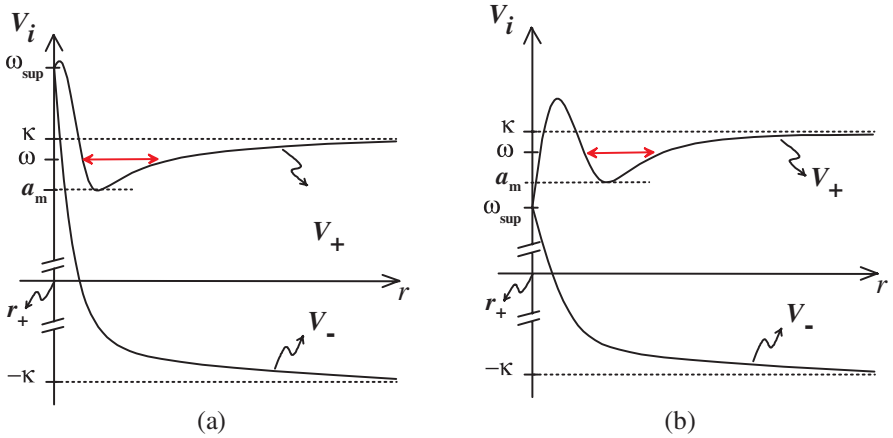

FIG. 2 (color online). (a) Qualitative shape of the potentials V_+ and V_- for a boosted Kerr black string in which an instability is present. An example of data that yields this kind of potentials is $(2M = 1, a = 0.499\,999, \tanh\sigma = 1/\sqrt{2}, \kappa = 1.85, l = m = 1)$. Potentially unstable modes are those whose frequency satisfies $a_{\rm m} < \omega < \kappa$. Thus, they are bound states of the potential well in V_+ that satisfy the superradiant condition $\omega < \omega_{\rm sup}$. (b) Qualitative shape of the potentials V_+ and V_- for a case in which the Kerr black string is stable. An example of data that yields this kind of potentials is $(2M = 1, a = 0.4, \tanh\sigma = 1/\sqrt{2}, \kappa = 1.85, l = m = 1)$. The bound state modes with $a_{\rm m} < \omega < \kappa$ are stable because they do not satisfy the superradiant condition $\omega < \omega_{\rm sup}$, where $\omega_{\rm sup}$ is defined in (25).

(forbidden regions), the solutions have a real exponential behavior. In both Figs. 2(a) and 2(b), the potential V_+ has a well that is limited at infinity by the KK momentum potential barrier of height κ. Modes with a frequency greater than the bottom of the well, $a_{\rm m}$, and smaller than κ, $a_{\rm m} < \omega < \kappa$, are bound states. If these bound state frequencies further satisfy the superradiant condition (26), an instability will settle down: the waves will bounce back and forth between the KK wall at infinity and the black hole, amplifying itself each time [Fig. 2(a)]. If the bound state frequencies do not satisfy the superradiant condition (26) the modes will bounce back and forth in the potential well, but each time part of the wave will tunnel to the horizon until the full mode is completely absorbed by the horizon [Fig. 2(b)].

Here we note that when we set the rotation parameter to zero, $a = 0$ (boosted Schwarzschild black string), we always get potentials of the form represented in Fig. 2(b), for any M, σ and κ, l, m. In particular, this means that the bound states of the boosted black string are always damped modes since the superradiant condition (26) is never satisfied. This was first noticed in [27,33], where it was shown that superradiant scattering is never possible in a boosted Schwarzschild black string, although the particle analogue of this phenomena—the Penrose process—can occur. Ultimately, this is because one can construct, with a combination of $\partial/\partial t$ and $\partial/\partial z$, a Killing vector field that is everywhere timelike outside the horizon [39].

The KK momentum is a necessary condition for the existence of bound states, but is not a sufficient condition as we shall see in Sec. V, where we will conclude that the Myers-Perry black string is stable due to the lack of bound states.

IV. FREQUENCY SPECTRUM: INSTABILITY TIME SCALE

In the last section we concluded that some boosted Kerr black strings are unstable to scalar field perturbations that might develop in the vicinity of the horizon, and we identified the relevant ingredients for this process. However, we still do not know the quantitative features of the instability, namely, we do not know the allowed spectrum of real frequencies of the bound states, and what the instability time scale is.

In this section we will address these issues. The method we shall use here, known as matched asymptotic expansion, has been widely used with success for the computation of the scattering cross section of black holes [40], and also for computing instabilities in the Kerr background [17–19]. We will assume that the Compton wavelength of the scalar particle is much larger than the typical transverse size of the black string; we divide the space outside the event horizon into two regions, namely, a near region and a far region. These two regions have an overlapping region where we can match their wave solutions to get a solution to the problem. This allows the analysis of the instability properties. When the correct boundary conditions are imposed, namely, only ingoing flux at the horizon and only outgoing waves at infinity, we get a defining equation for ω. The stability or instability of the spacetime depends basically on the sign of the imaginary component of ω.

A. The near-region solution

First, let us focus on the near region in the vicinity of the horizon, $r - r_+ \ll 1/\omega$. We work in the regime $\omega^2 r_+^2 \ll 1$,

$\omega^2 a^2 \ll 1$, $\kappa^2 r_+^2 \ll 1$ and σ not too large (which is definitely the case for balanced rings), and define the new variable

$$y = \frac{r - r_+}{r - r_-}, \tag{29}$$

whose range is $0 \leq y \leq 1$. The horizon is at $y = 0$ and infinity is at $y = 1$. We have $\Delta = (r_+ - r_-)^2 y/(1-y)^2$, $\Delta\,\partial_r = (r_+ - r_-) y \partial_y$. In the near region and in the regime in which we work, we can neglect the contribution of the terms coming from $\kappa^2 r^2 + a^2\omega^2 - 2\omega m a \cosh\sigma$ in (19), when comparing them with $\lambda_{ml} \simeq l(l+1)$. In this case we can find an analytical near-horizon solution for the wave equation. More concretely, in the near region, the radial wave equation (19) can then be written as

$$y(1-y)\partial_y^2\Psi + (1-y)\partial_y\Psi + \left[-\frac{l(l+1)}{1-y} + \frac{1-y}{y}\varpi^2\right]\Psi = 0, \tag{30}$$

where we have introduced the superradiant factor ϖ as defined in (24). Through the definition

$$\Psi = z^{i\varpi}(1-y)^{l+1}F, \tag{31}$$

the near-region radial wave equation becomes

$$y(1-y)\partial_y^2 F + [(1 + i2\varpi) - [1 + 2(l+1) + i2\varpi]y]\partial_y F - [(l+1)^2 + i2\varpi(l+1)]F = 0. \tag{32}$$

This wave equation is a standard hypergeometric equation [41] of the form

$$y(1-y)\partial_y^2 F + [c - (a+b+1)y]\partial_y F - abF = 0, \tag{33}$$

with

$$a = l + 1 + i2\varpi, \qquad b = l + 1, \qquad c = 1 + i2\varpi. \tag{34}$$

The general solution of this equation in the neighborhood of $z = 0$ is $Ay^{1-c}F(a-c+1, b-c+1, 2-c, y) + BF(a, b, c, y)$. Using (31), one finds that the most general solution of the near-region equation is

$$\Psi = Ay^{-i\varpi}(1-y)^{l+1}F(a-c+1, b-c+1, 2-c, y) + By^{i\varpi}(1-y)^{l+1}F(a, b, c, y). \tag{35}$$

The first term represents an ingoing wave at the horizon $y = 0$, while the second term represents an outgoing wave at the horizon [recall the discussion after (26)]. We are working at the classical level, so there can be no outgoing flux across the horizon, and thus one sets $B = 0$ in (35). Note that one then gets the near-horizon solution written in (23). Later on, to do the matching between the near and far regions, we will be interested in the large r, $y \to 1$, behavior of the ingoing near-region solution. To achieve this aim one uses the $y \to 1 - y$ transformation law for the hypergeometric function [41],

$$\begin{aligned} F(a-c+1, b-c+1, 2-c, y) &= (1-y)^{c-a-b}\frac{\Gamma(2-c)\Gamma(a+b-c)}{\Gamma(a-c+1)\Gamma(b-c+1)} \\ &\quad \times F(1-a, 1-b, c-a-b+1, 1-y) \\ &\quad + \frac{\Gamma(2-c)\Gamma(c-a-b)}{\Gamma(1-a)\Gamma(1-b)}F(a-c+1, \\ &\quad b-c+1, -c+a+b+1, 1-y), \end{aligned} \tag{36}$$

and the property $F(a, b, c, 0) = 1$. The large r behavior of the ingoing wave solution in the near region is then given by

$$\Psi \sim A\Gamma(1 - i2\varpi)\left[\frac{(r_+ - r_-)^{-l}\Gamma(2l+1)}{\Gamma(l+1)\Gamma(l+1-i2\varpi)}r^l + \frac{(r_+ - r_-)^{l+1}\Gamma(-2l-1)}{\Gamma(-l)\Gamma(-l-i2\varpi)}r^{-l-1}\right]. \tag{37}$$

B. The far-region solution

In the far region, $r - r_+ \gg r_+$, and for $\omega a \ll 1$, the wave equation (19) reduces to

$$\partial_r^2(r\Psi) + \left[\omega^2 - \kappa^2 + \frac{r_+ + r_-}{r}(\omega\sinh\sigma - \kappa\cosh\sigma)^2 - \frac{l(l+1)}{r^2}\right](r\Psi) = 0. \tag{38}$$

If we define

$$\eta^2 \equiv \kappa^2 - \omega^2, \qquad \rho \equiv \frac{(r_+ + r_-)(\omega\sinh\sigma - \kappa\cosh\sigma)^2}{2\eta}, \qquad \chi = 2\eta r, \tag{39}$$

Eq. (38) is written as

$$\partial_\chi^2(\chi\Psi) + \left[-\frac{1}{4} + \frac{\rho}{\chi} - \frac{l(l+1)}{\chi^2}\right](\chi\Psi) = 0. \tag{40}$$

This is a standard Wittaker equation [41], $\partial_\chi^2 W + [-\frac{1}{4} + \frac{\rho}{\chi} - \frac{1-\mu^2}{\chi^2}]W = 0$, with

$$W = \chi\Psi, \qquad \mu = l + 1/2. \tag{41}$$

The most general solution of this equation is $W = \chi^{\mu+1/2}e^{-\chi/2}[\alpha M(\tilde{a}, \tilde{b}, \chi) + \beta U(\tilde{a}, \tilde{b}, \chi)]$, where M and U are the Wittaker's functions with $\tilde{a} = 1/2 + \mu - \rho$ and $\tilde{b} = 1 + 2\mu$. In terms of the parameters that appear in (40) one has

$$\tilde{a} = l + 1 - \rho, \qquad \tilde{b} = 2l + 2. \tag{42}$$

The far-region solution of (40) is then given by

$$\Psi = \alpha\chi^l e^{-\chi/2} M(\tilde{a}, \tilde{b}, \chi) + \beta\chi^l e^{-\chi/2} U(\tilde{a}, \tilde{b}, \chi). \quad (43)$$

To impose the boundary condition at infinity, we will need to know the behavior of the far-region solution at the large $\chi = 2\eta r \to \infty$ regime. When $\chi \to +\infty$, one has $U(\tilde{a}, \tilde{b}, \chi) \sim \chi^{-\tilde{a}}$ and $M(\tilde{a}, \tilde{b}, \chi) \sim \chi^{\tilde{a}-\tilde{b}} e^{\chi} \Gamma(\tilde{b})/\Gamma(\tilde{a})$ [41], and thus, for large χ, the far-region solution behaves as

$$\Psi \sim \alpha \frac{\Gamma(2l+2)}{\Gamma(l+1-\rho)} \chi^{-1-\rho} e^{\chi/2} + \beta\chi^{-1+\rho} e^{-\chi/2}. \quad (44)$$

It is clear that the first term proportional to $e^{+\chi/2}$ represents an ingoing wave, while the second term proportional to $e^{-\chi/2}$ represents an outgoing wave. At this point we can finally discuss the second boundary condition of our problem. In our present experiment, one perturbs the boosted Kerr black string outside its horizon, and this generates a wave that propagates both into the horizon and out to infinity. Therefore, at $r \to +\infty$, our physical system has only an outgoing wave, and thus one has to set $\alpha = 0$ in (43) and (44). The behavior of the solution at infinity then boils down to (23). We can understand this boundary condition in an alternative way. As we are already anticipating with the definition chosen for η^2 in (39) the unstable modes will be those with $\omega < \kappa$, i.e., whose frequency is smaller than the potential barrier at infinity. At infinity the wave mode will then have a *real* exponential behavior, $\Psi \sim e^{\pm\chi}$, and the requirement of regularity at infinity amounts to discarding the solution $e^{+\chi}$ that diverges at infinity. This is done by setting $\alpha = 0$.

C. Matching condition: Frequency spectrum

In this subsection we shall find the real frequencies that are allowed to propagate in the boosted Kerr black string background, and we will use the matching of the far and near regions in their overlapping sector to select the imaginary part of the mode frequencies.

We begin by asking what the (real) frequencies are that can propagate in the background of the boosted Kerr black string. To do so, we shall use a trick [18] that was already applied with success to solve similar problems in the background of a Kerr black hole [18], of a Kerr black string [21], and of a boosted Schwarzschild black string [27]. That this method yields indeed the correct answer has already been confirmed by a full numerical checking.[1] We assume for a moment that we have no black hole, and we ask what the frequencies are that can propagate in this horizon-free background. In this setup, we are actually looking for the pure normal modes that can propagate in a geometry that is horizon-free and that have a reflecting spherical wall produced by the effective mass of the extra dimension. In this geometry, the wave solution of the Klein-Gordon equation is everywhere described by (43), subjected to the appropriate boundary conditions. The outer boundary condition requires the presence of only outgoing waves and this implies $\alpha = 0$. The inner boundary condition is that Ψ must be regular at the origin, $\chi \to 0$. For small values of χ, the solution is described by $\Psi \sim \beta[\Gamma(2l+1)/\Gamma(l+1-\rho)](2\eta r)^{-l-1}$ [41]. So, when $\chi \to 0$, the wave function Ψ diverges, $r^{-l-1} \to \infty$. To have a regular solution there, we must then demand that $\Gamma(l+1-\rho) \to \infty$. This occurs when the argument of the gamma function is a nonpositive integer, $\Gamma(-N) = \infty$ with $N = 0, 1, 2, \cdots$. Therefore, the requirement of regularity imposes the condition $l + 1 - \rho = -N$. Since ρ is related to ω, the above regularity demanding amounts to a natural selection of the allowed frequencies that can propagate in the geometry.

Now, let us come back to the boosted Kerr black string background, which differs clearly from the above background due to the existence of a horizon. In the spirit of [18,19], we expect that the presence of a horizon induces a small complex imaginary part in the allowed frequencies, $\omega_i = \mathrm{Im}[\omega]$, that describes the slow decay of the amplitude of the wave if $\omega_i < 0$, or the slowly growing instability of the mode if $\omega_i > 0$. Now, from (39), one sees that a frequency ω with a small imaginary part corresponds to a complex ρ with a small imaginary part that we will denote by $\delta\rho \equiv \mathrm{Im}[\rho]$. Therefore, we anticipate that in the boosted Kerr black string one has

$$\rho = (l + 1 + N) + i\delta\rho, \quad (45)$$

with N being a non-negative integer, and $\delta\rho$ being a small quantity. In particular, this means that, onwards, the arguments of the Wittaker's function $U(\tilde{a}, \tilde{b}, \chi)$ previously defined in (42) are to be replaced by

$$\tilde{a} = -N - i\delta\rho, \qquad \tilde{b} = 2l + 2. \quad (46)$$

What we have done so far is to find the spectrum of real frequencies. To find the imaginary part of the modes, we have to match the far region with the near region. So, we need to find the small χ behavior of the far-region solution (43). The Wittaker's function $U(\tilde{a}, \tilde{b}, \chi)$ can be expressed in terms of the Wittaker's function $M(\tilde{a}, \tilde{b}, \chi)$ [41]. Inserting this relation in (43), the far-region solution can be written as

[1] We can do the analysis without making use of this trick. Indeed, we can find an algebraic equation for the spectrum of real frequencies and the instability time scale just by using the second relation of (39), with $\rho = \mathrm{Re}[\rho] + i\delta\rho$, and $\delta\rho$ given by (50), and without using (45). However, this trick clarifies the physical nature of the real frequencies, and yields the right answer, as a full numerical analysis of the unboosted case confirms [22].

TABLE I. Some numerical values of the instability as we vary the rotation parameter a of a geometry with $2M = 1$, $\sigma = \mathrm{arctanh}(1/\sqrt{2})$, and for modes with $\kappa = 0.5$ and $l = m = 1$, $N = 0$. In the second and third columns we have, respectively, the real part, $\mathrm{Re}[\omega]$, and the imaginary part, $\mathrm{Im}[\omega]$, of the mode frequency. In the fourth column we present the superradiant factor ϖ multiplied by $4\pi T_H$. The unstable modes have $\mathrm{Im}[\omega] > 0$ and are those that satisfy simultaneously $\varpi < 0$ and $\omega < \kappa$. The last three columns show the values of the quantities that must be small in the regime of validity of our results, namely, $a^2(\kappa^2 - \omega^2) \ll 1$, $\omega a \ll 1$ and $\kappa^2 r_+^2 \ll 1$. Note that the condition $\omega^2 r_+^2 \ll 1$ is automatically satisfied when $\kappa^2 r_+^2 \ll 1$, since the unstable modes we are dealing with are those that have $\omega < \kappa$.

a	$\mathrm{Re}[\omega]$	$\mathrm{Im}[\omega]$	$4\pi T_H \varpi$	$a^2(\kappa^2 - \omega^2)$	ωa	$\kappa^2 r_+^2$
0.198	0.499 885	-3.90×10^{-14}	+0.0004	4×10^{-6}	0.10	0.23
0.199	0.499 885	4.85×10^{-14}	−0.0004	4×10^{-6}	0.10	0.23
0.200	0.499 885	1.36×10^{-13}	−0.0012	4×10^{-6}	0.10	0.23
0.300	0.499 885	7.50×10^{-12}	−0.0894	1×10^{-5}	0.15	0.20
0.400	0.499 885	1.29×10^{-11}	−0.2072	2×10^{-5}	0.20	0.16
0.450	0.499 885	1.59×10^{-11}	−0.2969	2×10^{-5}	0.22	0.13
0.490	0.499 885	2.00×10^{-11}	−0.4316	3×10^{-5}	0.24	0.09
0.499	0.499 885	2.26×10^{-11}	−0.5174	3×10^{-5}	0.25	0.07

$$\Psi = \beta \chi^l e^{-\chi/2} \frac{\pi}{\sin(\pi \tilde{b})} \left[\frac{M(\tilde{a}, \tilde{b}, \chi)}{\Gamma(1 + \tilde{a} - \tilde{b})\Gamma(\tilde{b})} - \chi^{1-\tilde{b}} \frac{M(1 + \tilde{a} - \tilde{b}, 2 - \tilde{b}, \chi)}{\Gamma(\tilde{a})\Gamma(2 - \tilde{b})} \right], \tag{47}$$

with $\tilde{a}$ and $\tilde{b}$ defined in (46). Now, we want to find the small χ behavior of (47), and to extract $\delta\rho$ from the gamma function. This is done in (A1)–(A3), yielding for small $\delta\rho$ and for small χ the result

$$\Psi \sim \beta(-1)^N \frac{(2l + 1 + N)!}{(2l + 1)!} (2\eta r)^l + \beta(-1)^{N+1} \times (2l)! N! (i\delta\rho)(2\eta r)^{-l-1}. \tag{48}$$

The quantity $\delta\rho$ cannot take any value. Its allowed values are selected by requiring a match between the near-region solution (37) and the far-region solution (48). So, the allowed values of $\delta\rho$ are those that satisfy the matching condition

$$- i\delta\rho \frac{(2l)!(2l + 1)! N!}{(2l + N + 1)!(2\eta)^{2l+1}} = (r_+ - r_-)^{2l+1} \frac{\Gamma(l + 1)}{\Gamma(2l + 1)} \frac{\Gamma(-2l - 1)}{\Gamma(-l)} \times \frac{\Gamma(l + 1 - i2\varpi)}{\Gamma(-l - i2\varpi)}. \tag{49}$$

Use of the gamma function relations (A4) yields

$$\delta\rho = -2\varpi [2\eta(r_+ - r_-)]^{2l+1} \frac{(2l + 1 + N)!}{N!} \times \left[\frac{l!}{(2l)!(2l + 1)!} \right]^2 \prod_{j=1}^{l} (J^2 + 4\varpi^2), \tag{50}$$

for $l \geq 1$, while for $l = 0$ one gets

$$\delta\rho = -4\eta(r_+ - r_-)(N + 1)\varpi. \tag{51}$$

Condition (45) together with (39) leads to

TABLE II. Some numerical values of the instability for a geometry with $2M = 1$, $a = 0.35$, $\sigma = \mathrm{arctanh}(1/\sqrt{2})$, and for modes with $l = m = 1$, $N = 0$ and several values of the KK momentum κ. In the second and third columns we have, respectively, the real part, $\mathrm{Re}[\omega]$, and the imaginary part, $\mathrm{Im}[\omega]$, of the mode frequency. In the fourth column we present the superradiant factor ϖ multiplied by $4\pi T_H$. The unstable modes have $\mathrm{Im}[\omega] > 0$ and are those that satisfy simultaneously $\varpi < 0$ and $\omega < \kappa$. The last three columns show the values of the quantities that must be small in the regime of validity of our results.

κ	$\mathrm{Re}[\omega]$	$\mathrm{Im}[\omega]$	$4\pi T_H \varpi$	$a^2(\kappa^2 - \omega^2)$	ωa	$\kappa^2 r_+^2$
0.01	0.009 99	1.67×10^{-26}	−0.285	2×10^{-12}	0.004	0.0007
0.10	0.099 99	1.38×10^{-17}	−0.259	2×10^{-8}	0.04	0.01
0.30	0.299 98	1.74×10^{-13}	−0.201	2×10^{-6}	0.10	0.07
0.50	0.499 88	1.04×10^{-11}	−0.142	1.4×10^{-5}	0.18	0.18
0.70	0.699 68	1.11×10^{-10}	−0.084	5×10^{-5}	0.25	0.36
0.90	0.899 32	3.10×10^{-10}	−0.026	2×10^{-4}	0.31	0.59
1.00	0.999 07	-9.90×10^{-11}	+0.003	2×10^{-4}	0.35	0.73

$$\frac{(r_+ + r_-)(\omega \sinh\sigma - \kappa \cosh\sigma)^2}{2\sqrt{\kappa^2 - \omega^2}} = l + N + 1 + i\delta\rho, \tag{52}$$

with $\delta\rho$ given by (50). This is an algebraic equation for the characteristic values of the frequency ω. All these values must be consistent with the assumptions made, namely, (20), (30), and (38) are valid only for $a^2(\kappa^2 - \omega^2) \ll 1$, $\omega a \ll 1$ and $\kappa^2 r_+^2 \ll 1$. If ω has a positive imaginary part, then the mode is unstable. Indeed, the field has the time dependence $e^{-i\omega t}$, so a positive imaginary part for ω means the amplitude grows exponentially as time goes by. We have indeed found unstable modes. Representative elements of this class of modes are displayed in Table I (where we fix the Kaluza-Klein momentum κ of the mode and vary the rotation a of the geometry) and in Table II (where we fix a and vary κ). As a consistency check, in Appendix B, we show that, when we turn off the boost, (52) yields the result found originally by Detweiler [18].

We discuss the results in Sec. VI.

V. STABILITY ANALYSIS OF THE BOOSTED MYERS-PERRY BLACK STRING

The boosted Myers-Perry black string can also be constructed by adding a flat direction z to the Myers-Perry black hole [2],[2] and then applying a Lorentz boost to it, $dt \to \cosh\sigma dt + \sinh\sigma dz$ and $dz \to \sinh\sigma dt + \cosh\sigma dz$. The geometry of a boosted Myers-Perry black string geometry is then (for our purposes it is enough to consider the case with rotation in a single plane parametrized by ϕ)

$$\begin{aligned} ds^2 = &-\left(1 - \frac{2Mr^{1-n}\cosh^2\sigma}{\Sigma}\right)dt^2 + \frac{2Mr^{1-n}\sinh(2\sigma)}{\Sigma}dtdz \\ &+ \left(1 + \frac{2Mr^{1-n}\sinh^2\sigma}{\Sigma}\right)dz^2 + \frac{\Sigma}{\Delta}dr^2 + \Sigma d\theta^2 \\ &+ \frac{(r^2+a^2)^2 - \Delta a^2\sin^2\theta}{\Sigma}\sin^2\theta d\phi^2 \\ &- \frac{4Mr^{1-n}\cosh\sigma}{\Sigma}a\sin^2\theta dt d\phi \\ &- \frac{4Mr^{1-n}\sinh\sigma}{\Sigma - 2Mr^{1-n}}a\sin^2\theta dz d\phi + r^2\cos^2\theta d\Omega_n^2, \end{aligned} \tag{53}$$

where $n = D - 4$, $d\Omega_n^2$ describes the line element of a unit n sphere, and

$$\Delta = r^2 + a^2 - 2Mr^{1-n}, \qquad \Sigma = r^2 + a^2\cos^2\theta. \tag{54}$$

Under the separation ansatz

$$\Phi = e^{-i\omega t}e^{im\phi}e^{-i\kappa z}S_l^m(\theta)\Psi(r)Y(\Omega), \tag{55}$$

the Klein-Gordon equation yields the following angular and radial wave equations for $S_l^m(\theta)$ and $\Psi(r)$,

$$\begin{aligned} &\frac{1}{\sin\theta\cos^n\theta}\partial_\theta(\sin\theta\cos^n\theta\,\partial_\theta S_l^m) + \Bigg[a^2(\omega^2 - \kappa^2)\cos^2\theta \\ &\quad - \frac{m^2}{\sin^2\theta} + \lambda_{lm} - \frac{j(j+n-1)}{\cos^2\theta}\Bigg]S_l^m = 0, \end{aligned} \tag{56}$$

$$\frac{\Delta}{r^n}\partial_r(r^n\Delta\,\partial_r\Psi) + U\Psi = 0, \tag{57}$$

where λ_{lm} is the (n-dimensional) separation constant given by $\lambda_{lm} = l(l+1+n) + \mathcal{O}(a^2(\omega^2 - \kappa^2))$, and

$$\begin{aligned} U = -\Delta\Bigg[&\kappa^2 r^2 + a^2\omega^2 - 2\omega ma\cosh\sigma + \lambda_{lm} \\ &+ j(j+n-1)\frac{a^2}{r^2}\Bigg] + [[\omega(r^2+a^2) - ma\cosh\sigma]^2 \\ &+ 2Mr^{1-n}(r^2+a^2)\cosh^2\sigma[\omega - \kappa\tanh\sigma]^2 \\ &- 2Mr^{1-n}(r^2+a^2)\omega^2 - m^2a^2\sinh^2\sigma \\ &+ 4\kappa maMr^{1-n}\sinh\sigma]. \end{aligned} \tag{58}$$

In (56) and (58), the integer $m = 0, \pm1, \pm2, \cdots$ comes from separation of the angle describing the azimuthal dependence of the perturbations around the symmetry axis [see (55)]. The terms dependent on n and the parameter $j = 0, 1, 2, \cdots$ are the eigenvalues of the hyperspherical harmonics on the n sphere, which are given by $-j(j+n-1)$ [42]. The integer l is constrained to satisfy the condition $l \geq (j + |m|)$. Note that (56)–(58) reduce to (18) and (19) when we set simultaneously $n = 0$ and $j = 0$.

The boundary conditions are only ingoing flux at the horizon and only outgoing waves at infinity,

$$\Psi(r) \sim \begin{cases} (r - r_+)^{-i\varpi} = e^{-i\varpi\ln(r-r_+)}, & \text{as } r \to r_+, \\ r^{-(n+2)/2}e^{+i\sqrt{\omega^2-\kappa^2}r}, & \text{as } r \to \infty, \end{cases} \tag{59}$$

where

$$\varpi = \frac{r_+(r_+^2 + a^2)\cosh\sigma}{(n+2)r_+^2 + (n-1)a^2}(\omega - \omega_{\text{sup}}), \tag{60}$$

with ω_{sup} defined in (25).

Defining the tortoise coordinate r_* and a new wave function χ as

$$dr_* = \frac{r_+^2 + a^2}{\Delta}dr, \qquad \Psi = [(r_+^2 + a^2)r^n]^{-1/2}\chi, \tag{61}$$

the radial wave equation (57) can be written in the form of an effective Schrödinger equation,

$$\partial_{r_*}^2\chi - V\chi = 0, \tag{62}$$

with

[2]The Myers-Perry black hole lives in a background with $D \geq 5$ spacetime dimensions. The corresponding black string lives in a $(D+1)$-dimensional background.

$$V = -\frac{U}{(r^2+a^2)^2} + G^2 + \partial_{r_*} G, \qquad G = \frac{1}{2}\partial_{r_*}\ln[(r_+^2+a^2)r^n]. \tag{63}$$

For $a^2(\omega^2-\kappa^2) \ll 1$ one has $\lambda_{lm} \approx l(l+1+n)$ and V is then a quadratic function of ω that can be factorized as

$$V = -\gamma(\omega - V_+)(\omega - V_-), \tag{64}$$

with

$$\gamma = \frac{r^{1-n}}{(r^2+a^2)^2}[r^{1+n}(r^2+a^2) + 2M(r^2\sinh^2\sigma + a^2\cosh^2\sigma)] > 0,$$
$$V_\pm = -\frac{V_1}{2\gamma} \pm \sqrt{\left(\frac{V_1}{2\gamma}\right)^2 - \frac{V_0}{\gamma}}, \tag{65}$$

and

$$V_0 = -\frac{j(j+n-1)a^2\Delta}{r^2(r^2+a^2)^2} + \frac{-[\kappa^2 r^2 + l(l+1+n)]\Delta + m^2a^2 + 4\kappa amMr^{1-n}\sinh\sigma}{(r^2+a^2)^2} + \frac{2M\kappa^2 r^{1-n}\sinh^2\sigma}{r^2+a^2}$$
$$- \frac{r^{-n-2}\Delta}{4(r^2+a^2)^4}[n(n-2)a^6r^n + (n+2)r^5[2M(n+2)+nr^{1+n}] + a^4r[2Mn^2 + (3n^2-2n+4)r^{1+n}]$$
$$+ a^2r^3[4M(n^2+2n-4) + (3n^2+2n+4)r^{1+n}]],$$
$$V_1 = -\frac{4Mr^{1-n}\cosh\sigma[ma + \kappa\sinh\sigma(r^2+a^2)]}{(r^2+a^2)^2}. \tag{66}$$

Important features of γ and $V_\pm$ are their asymptotic values at the horizon and infinity which are given by

$$\lim_{r\to r_+}\gamma = \cosh^2\sigma, \qquad \lim_{r\to\infty}\gamma = 1,$$
$$\lim_{r\to r_+} V_\pm = \omega_{\rm sup}, \qquad \lim_{r\to\infty} V_\pm = \pm|\kappa|. \tag{67}$$

Note that when $n = 0$ (which implies $j = 0$), the relations of this section yield the potentials discussed in Sec. III C. In this case, we have already analyzed the potentials $V_\pm$ in Figs. 2(a) and 2(b). For $n \geq 1$, the relevant features of the potentials are independent of n, and significantly different from the $n = 0$ case. The only two kinds of potentials that can occur for $n \geq 1$ are drawn in Figs. 3(a) and 3(b). Superradiant modes are allowed [Fig. 3(a)], but the KK momentum is never able to generate a potential well, i.e., bound states, and thus the superradiant instability does not develop. When we set the boost to zero, $\sigma = 0$, our results and graphs reduce to the ones found in [22,43].

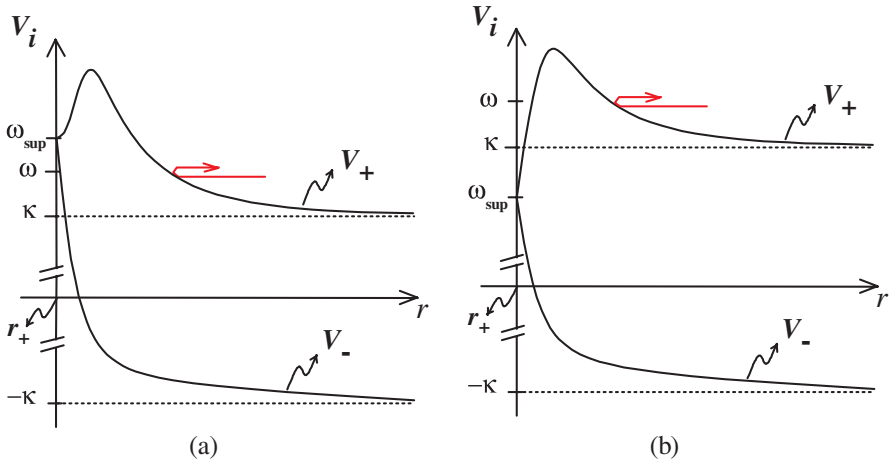

FIG. 3 (color online). (a) General qualitative shape of the potentials V_+ and V_- for a boosted Myers-Perry black string. In this case the geometry is always stable, but superradiant scattering is possible. An example of data that yields this kind of potentials is ($2M = 1$, $a = 0.9$, $\tanh\sigma = 1/\sqrt{2}$, $\kappa = 1.5$, $l = m = 1$, $j = 0$, $n = 1$). There are no bound state modes since V_+ approaches κ at infinity from above. This absence of bound states for $n \geq 1$, as opposed to the $n = 0$ case, annihilates the possibility of an instability existing for $n \geq 1$. Since $\omega < \omega_{\rm sup}$, superradiant scattering is possible. (b) Qualitative shape of the potentials V_+ and V_- for a Myers-Perry black string. In this case the geometry is stable, and moreover superradiant scattering is not possible. An example of data that yields this kind of potentials is ($2M = 1$, $a = 0.5$, $\tanh\sigma = 1/\sqrt{2}$, $\kappa = 2$, $l = m = 1$, $j = 0$, $n = 1$). There are no bound state modes and superradiant scattering is not possible (since $\omega > \omega_{\rm sup}$).

As pointed out in [22], this absence of instability in the $n \geq 0$ case seems to be related with the fact that, at least for $n = 1$, there are no stable circular orbits [44].

We end this section with a remark on the value of the boost angle for $n \geq 1$. As is being assumed in this section, if black rings exist in six and higher dimensions, their infinite-radius limit will be a boosted Myers-Perry black string. However, the balanced rings need not give boosted strings with $\tanh\sigma = 1/\sqrt{2}$ (the value for the Kerr black string). Presumably, but we do not know for sure, the balanced rings give pressureless boosted black strings. To find the relevant value for σ in the higher-dimensional case one would have to solve the equation $T_{zz} = 0$, where T_{zz} will be defined in (69). The result for σ may therefore depend on the dimension of the spacetime. We have tested several values of σ and verified that we always get potentials like the ones plotted in Fig. 3 that show no evidence of superradiant instability.

VI. DISCUSSION OF THE RESULTS: THE INSTABILITY END POINT—BOUND MECHANISM FOR THE ROTATION

We have shown that the 5D large radius doubly spinning black rings are unstable against superradiant bound modes. The most physically intuitive method to identify the nature of the instability is to write the radial wave equation as a Schrödinger equation and to look to the factorized Schrödinger potentials, as was done in Sec. III C. When the instability is present the potentials are like the ones drawn in Fig. 2(a). The two ingredients necessary for the activation of the instability are the existence of a potential well in V_+ that can trap bound states, and that superradiance is present. In the boosted Kerr black string ($n = 0$) these two ingredients can be simultaneously present. Therefore, the large radius 5D black rings are unstable against this mechanism. We also note that there are, in addition, damped modes which are bound states that do not suffer superradiance and die off through the tunneling to the horizon, as shown in Fig. 2(b).

To find the frequency spectrum of the unstable modes and the time scale of the process, we have used the matched asymptotic method. The main features of the instability found for the large radius black ring solution (the boosted Kerr black string) can be summarized as follows:

(i) In Table I we show the evolution of the instability when the rotation a of the boosted Kerr black string increases, while keeping all other parameters of the geometry and angular parameters of the mode fixed. We see that the instability is robust and it gets stronger (the time scale $\tau \sim 1/\mathrm{Im}[\omega]$ decreases) when the rotation a increases. There is a natural explanation for this behavior. The instability is triggered by superradiance which is present only when the background rotates. Therefore we expect the superradiance and thus the instability to be stronger when the rotation is bigger: in Table I, one sees that as a increases so does $|\varpi|$ and $\mathrm{Im}[\omega]$.

(ii) Climbing Table II from the bottom to the top we verify that a transition from an unstable situation to a stable one occurs between the second and first line. This happens because below a critical rotation the superradiant condition $\mathrm{Re}[[\omega] < \kappa\tanh\sigma + m\Omega_\phi\cosh^{-2}\sigma$ is no longer valid, and it clearly identifies superradiance as the mechanism responsible for the instability.

(iii) In Table II we show the evolution of the instability when the KK momentum κ of the mode increases, while keeping all other parameters of the geometry and angular parameters of the mode fixed. In general, the instability is robust and it gets stronger when κ increases. This behavior can be understood by noting that the potential well of V_+ in Fig. 2(a) gets deeper when κ increases. Thus, the bound modes get more efficiently trapped in the well.

(iv) However, when κ increases above a critical value the superradiant condition $\mathrm{Re}[\omega] < \kappa\tanh\sigma + m\Omega_\phi\cosh^{-2}\sigma$ is no longer valid and the instability stops. This situation can be seen in the transition between the last two lines of Table II. Again, this is strong evidence that superradiance is the mechanism responsible for the instability.

(v) The most unstable mode we have found has a time scale $\tau \sim 1/\mathrm{Im}[\omega] \sim 10^7$, frequency $\mathrm{Re}[\omega] = 1.843\,98$, KK momentum $\kappa = 1.85$, and $l = m = 1$. This mode is present in the geometry $2M = 1$, $a = 0.499\,999$ and $\tanh\sigma = 1/\sqrt{2}$. The most unstable mode when there is no boost, $\sigma = 0$, has a time scale $\tau \sim 10^8$ [22]. Therefore the boost can considerably increase the strength of the instability.

(vi) When we set the rotation parameter to zero, $a = 0$ (boosted Schwarzschild black string), we always get potentials of the form represented in Fig. 2(b), for any M, σ and κ, l, m. In particular, this means that the bound states of the boosted black string are always damped modes since the superradiant condition (26) is never satisfied. This was first noticed in [27,33], where it was shown that superradiant scattering is never possible in a boosted Schwarzschild black string, although the particle analogue of this phenomena—the Penrose process—can occur.

We have shown that infinite-radius black rings have unstable scalar modes. However, we also expect gravitational unstable modes of the same kind to be present. Indeed, metric modes will also have KK momentum that provides the potential well that allows the existence of bound states, and it is well known that superradiant scattering also occurs for gravitational perturbations [37,40]. We thus have the ingredients for the development of the instability. Moreover this gravitational instability will be considerably stronger than the scalar one. Indeed, the

maximum superradiant amplification after each scattering is only 2% in the scalar case but it reaches 138% in the gravitational case [45].

A question that naturally arises whenever one has an instability is what is its end point. Quite often, this problem does not have a clear answer, the most paradigmatic example being the end point of the Gregory-Laflamme instability. The end point of the superradiant instability is, however, more predictable. Indeed, the amplitude of an unstable mode gets amplified during each scattering. The total energy of the system is conserved because the rotational energy of the boosted Kerr black string decreases during the process. Thus, the rotation a decreases as the instability evolves until it reaches the critical minimum value for which the superradiant factor ϖ vanishes (see the second item above). At this point the instability stops, and we have a black string with lower rotation than the initial one and some rotating radiation around it trapped in the potential well (that eventually escapes to infinity). This would be the full story if we only had one unstable mode with a specific value of κ, l, m. However, mode perturbations with several different values κ, l, m are spontaneously generated in the vicinity of the horizon. And the smaller the value κ of the unstable mode is, the smaller the minimum critical value of rotation, $a_{\rm crit}$, is for which superradiance (and the instability) ceases to operate, as indicated in Table III. Therefore we conclude that the several unstable modes will effectively spin down completely the boosted Kerr black string until its rotation along S^2 vanishes, and we are left with a boosted black string. Note, however, that Table III also tells us that, as the critical rotation decreases, the time scale of the unstable mode also gets significantly weaker. So the final stage of the complete spin down will take, in practice, a long time. Summarizing, a large radius doubly spinning black ring with rotation along both S^1 and S^2 will decay into a large radius black ring that rotates only along S^1.

We can ask if we can extend these results for black rings with finite radius. For example, it would be important to find out if the potential barrier of height κ at infinity is also present in small radius rings. To fully address this issue would require finding the line element of the doubly spinning black ring. Then, we would have to perform a full numerical analysis, since even when one of the rotations vanishes, the Klein-Gordon equation does not separate [27]. However, with the present knowledge, we can still partially address this question. Indeed, we can keep the approximation in which we use the boosted Kerr black string as a toy model for the doubly spinning black ring, but now we compactify the transverse direction, $z \sim z + 2\pi R$, and we slowly decrease R. In this case the KK momentum of a mode that propagates in the geometry gets quantized and can take only discrete values: $\kappa = \frac{k}{R}$, with k being an integer. This discretization of κ has important consequences. Indeed, now there is a minimum value for κ and thus there is a nonvanishing minimum for the critical rotation $a_{\rm crit}$ below which there is no superradiance and no instability. So we expect that a finite radius doubly spinning black ring will lose angular momentum along S^2 and will stabilize into a doubly spinning black ring with small, but nonvanishing, rotation along S^2. The superradiant instability will effectively impose an upper bound on the rotation along S^2. We can estimate the value of this upper bound. To stabilize the system, superradiance cannot be present, i.e., we must have $\varpi \geq 0$, with ϖ defined in (24). As we see in Tables I, II, and III, the unstable modes are waves with $\mathrm{Re}[\omega] \sim \kappa$. Therefore, in (24) we can replace the frequency by the KK momentum. Use of $\kappa = k/R$ yields that superradiance and hence the instability will be absent for black rings that satisfy the relation

$$R < k \cosh\sigma (1 - \tanh\sigma) \frac{r_+^2 + a^2}{ma}. \tag{68}$$

We can cast this relation in a more interesting form that gives an upper bound for the conserved angular momentum of the ring along S^2. To do so, we shall use the model of the black ring recently proposed by Hovdebo and Myers [15], with a small extension to accommodate a small angular momentum along S^2. The end point of the instability will have a small rotation along ϕ. It is then sufficient to work in the small a regime, for which one has $r_+^2 + a^2 \sim r_+^2$. The Hovdebo-Myers model assumes that the main features of a finite radius black ring can be reproduced by taking a loop of string with radius R and with an Arnowitt-Deser-Misner (ADM)-like stress tensor given by [46],

$$T_{ab} = \frac{1}{16\pi} \oint d\Omega_2 \hat{r}^2 n^i [\eta_{ab}(\partial_i h^c{}_c + \partial_i h^j{}_j - \partial_j h^j{}_i) - \partial_i h_{ab}], \tag{69}$$

TABLE III. The critical value for the rotation parameter, $a_{\rm crit}$, for which the superradiant factor vanishes, $\varpi \sim 0$, for three different values of κ. The other values not specified in the table are $2M = 1$, $\sigma = \mathrm{arctanh}(1/\sqrt{2})$, and $l = m = 1$, $N = 0$. For $a < a_{\rm crit}$, the instability is not active because superradiance is no longer present.

κ	$a_{\rm crit}$	$4\pi T_H \varpi$	$\mathrm{Re}[\omega]$	$\mathrm{Im}[\omega]$	$a^2(\kappa^2 - \omega^2)$	ωa	$\kappa^2 r_+^2$
0.50	$\sim$0.1985	$\sim 0^+$	0.499 88	4.79×10^{-15}	5×10^{-6}	0.099	0.23
0.10	$\sim$0.0414	$\sim 0^+$	0.099 99	2.44×10^{-21}	3×10^{-10}	0.004	0.01
0.01	$\sim$0.0043	$\sim 0^+$	0.009 99	6.28×10^{-30}	3×10^{-16}	0.000 04	0.0001

where $d\Omega_2$ is the line element of a 2-sphere, n^i is a radial unit vector in the transverse subspace, $\eta_{\mu\nu}$ is the flat space metric, and $h_{\mu\nu} = g_{\mu\nu} - \eta_{\mu\nu}$ is the deviation of the asymptotic metric from flat space. The index labels a, b, $c \in \{t, z\}$, while i, j run over the transverse directions. To apply this formula, the asymptotic metric must approach that of flat space in Cartesian coordinates. In the $a \ll r_+$ limit, this is accomplished by applying the coordinate transformation $r = \hat{r}[1 + r_+/(2\hat{r})]$ to (14) [15]. Using (69), one finds that the total energy, angular momentum along S^1, and angular momentum along S^2 are, respectively, given by

$$\begin{aligned} \hat{M} &= 2\pi R T_{tt} = \frac{\pi}{2} R r_+ (\cosh^2\sigma + 1), \\ \hat{J}_\psi &= 2\pi R^2 T_{tz} = \frac{\pi}{2} R^2 r_+ \cosh\sigma \sinh\sigma, \\ \hat{J}_\phi &= 2\pi R T_{t\phi} = \pi R r_+ a \cosh\sigma. \end{aligned} \tag{70}$$

Using these conserved charges we can rewrite (68) as

$$\hat{J}_\phi \lesssim \frac{k}{m}\left(\frac{r_+}{R}\right)^2 \left[R\left(\hat{M} - \frac{\pi r_+ R}{2}\right) - \hat{J}_\psi \right]. \tag{71}$$

Here, we confirm that for large radius rings the superradiant instability imposes $\hat{J}_\phi \to 0$. Note that (71) also suggests that $\hat{J}_\psi < R(\hat{M} - \frac{\pi r_+ R}{2})$. That is, doubly spinning black rings will also have an upper bound for the angular momentum along S^1, contrary to what happens with the black ring rotating only along S^1. This upper bound on $\hat{J}_\psi$ is present in dipole black rings rotating along S^1, and this is an indication that a similar case should occur in the doubly spinning black rings [8]. Relation (71) does not depend only on the conserved charges. The string model depends on four independent parameters, R, r_+, σ, and a, which correspond, respectively, to the size of the loop, thickness of the loop, tangential boost velocity along the loop, and rotation transverse to the loop [15]. The system (70) gives only three relations between the above four parameters for a fixed configuration of conserved charges. The fourth parameter is fixed by demanding that the ring acquires a configuration that maximizes its entropy [15]. This last quantity is computed using the area per unit length of the horizon, A_H, defined in (16). One finds that the entropy is given by $S = 2\pi R A_H/4 = 2\pi^2 R(r_+^2 + a^2) \times \cosh\sigma \sim 2\pi^2 R r_+^2 \cosh\sigma$, where the last approximation is valid in the small rotation regime. In the model of [15], it was found that this entropy is maximized for $\sigma = \sigma_{\max} \sim 0.709$. Use of (70) now allows us to write both r_+ and R as a function of the conserved charges. Then, the upper bound for the ADM angular momentum along S^2 can finally be written as

$$\hat{J}_\phi \lesssim 10^{-3}\pi\left(\frac{\hat{M}^2}{\hat{J}_\psi}\right)^3, \tag{72}$$

where we have set $k/m \sim 1$, since we do not expect high multipoles to be excited in a slowly rotating ring along ϕ. This is one of the main results of this paper. Basically, it is telling us that the instability provides a dynamical mechanism that bounds the rotation of the doubly spinning black ring along S^2.

It is important to note that the demand of a regular horizon in the yet to be found doubly spinning black ring will introduce a different upper bound for the rotation. The question is then whether the upper bound imposed dynamically by the instability is or is not smaller than the Kerr-like upper bound imposed by the existence of a regular horizon. To address this issue heuristically, and since $\hat{J}_\psi$ plays a minor role in this instability, we make use of the black ring that rotates along S^2 (see Sec. II B [11]). The comparison is more clear when the relations are written in terms of the parameters a and M. We first rewrite (71) in terms of a yielding $a/M \lesssim 2M/R$, in the limit $\sigma \sim 0$ and $a \ll r_+$. Next, we use the first relation of (13) in the first inequality of (11) to write the horizon bound as $a/M < 1$ (as expected, since in the large radius limit this is the Kerr bound). Therefore, for $2M/R \lesssim 1$, the instability plays an important role in the evolution of the solution, i.e., the instability will afflict large radius black rings but not small radius black rings.

Recently the existence of higher-dimensional black rings with horizon topology $S^1 \times S^{n+2}$, with $n = D - 4 > 0$ [47], has been conjectured. Evidence for this existence has already been given in [15], where a toy model for these objects was constructed. The large radius limit of these higher-dimensional black rings will naturally be a boosted Myers-Perry black string. We have searched for a similar instability in these geometries but we have found no superradiant instability. The stability of the Myers-Perry black string against this mechanism was established by Cardoso and Yoshida [22]. We have concluded that boosting the Myers-Perry black string does not change its superradiant stability. Again, the best way to understand the reason is to look to the Schrödinger-like wave equation and its factorized potentials, as was done in Sec. V. Although superradiance is still possible, the instability for $D > 5$ is not present because the KK momentum is not able to produce trapped bound states. This is clearly seen in the Schrödinger factorized potentials shown in Fig. 3(a). Again we can extend the analysis to black rings with finite radius. A similar reasoning as the one of the previous paragraph together with the absence of instability leads to the prediction that higher-dimensional doubly (multiply) spinning black rings will not have a superradiant upper bound for their rotations along S^{n+2}. The situation is somewhat similar to the Kerr/Myers-Perry black hole: the Kerr and 5D Myers-Perry solutions have an upper rotation bound but $D \geq 6$ Myers-Perry black holes do not. However, we expect that another dynamical process—the ultraspin mechanism [23]—might introduce a bound in the rotation.

It is also being conjectured that more general higher-dimensional black rings with other topologies rather than $S^1 \times S^{n+2}$ might exist [48]. An example would be a black object with topology $S^{(D-3)/2} \times S^{(D-1)/2}$ in odd D dimensions. In principle, the large radius limit of these multiply spinning black objects will be a boosted Myers-Perry membrane, i.e. (in the previous example), a $(\frac{D+3}{2})$-dimensional Myers-Perry black hole extended along $\frac{D-3}{2}$ flat boosted directions. These black rings will also be stable against superradiant bound modes since the KK contribution, due to the $(\frac{D-3}{2})$-brane on the wave equation, is not effectively different from the one coming from a single line. Indeed, the only difference in the potential (58) is that the KK massive term is $\kappa^2 = \sum \kappa_i^2$ with $i = 1, \cdots, (D-3)/2$, but this does not change the stability results [22].

ACKNOWLEDGMENTS

It is a pleasure to thank the participants of the KITP Program: "Scanning New Horizons: GR Beyond 4 Dimensions," and, in particular, Vitor Cardoso, Roberto Emparan, Donald Marolf, Robert Myers and Simon Ross for discussions and comments. Research at the Perimeter Institute is supported in part by funds from NSERC of Canada and MEDT of Ontario. I acknowledge financial support from Fundação para a Ciência e Tecnologia (FCT)–Portugal through Grant No. SFRH/BPD/2004, and from a NSERC Discovery grant through the University of Waterloo. I would also like to thank KITP and CENTRA for hospitality. This research was supported in part by the National Science Foundation under Grant No. PHY99-07949.

APPENDIX A: GAMMA FUNCTION RELATIONS

In this appendix we derive some gamma function relations that are used in the main body of the text.

(i) We start with the relations needed to extract $\delta\rho$ from the gamma functions that appear in (47) in order to get (48).
The properties $M(\tilde{a}, \tilde{b}, \chi = 0) = 1$ and $\Gamma(x)\Gamma(1-x) = \pi/\sin(\pi x)$ (with $x = \tilde{b} - \tilde{a}$ and then with $x = \tilde{b} - 1$) allow us to write (47) as

$$\Psi \sim \beta \chi^l e^{-\chi/2}\left[\frac{\sin[\pi(\tilde{b}-\tilde{a})]}{\sin(\pi\tilde{b})}\frac{\Gamma(\tilde{b}-\tilde{a})}{\Gamma(\tilde{b})} + \chi^{1-\tilde{b}}\frac{\Gamma(\tilde{b}-1)}{\Gamma(\tilde{a})}\right]. \tag{A1}$$

Use of (46) with $\delta\rho \sim 0$ yields

$$\frac{\sin[\pi(\tilde{b}-\tilde{a})]}{\sin(\pi\tilde{b})}\frac{\Gamma(\tilde{b}-\tilde{a})}{\Gamma(\tilde{b})} \sim (-1)^n \frac{(2l+1+n)!}{(2l+1)!}. \tag{A2}$$

To simplify the second term in between brackets in (A1), we use $\Gamma(\tilde{a})\Gamma(1-\tilde{a}) = \pi/\sin(\pi\tilde{a})$ with $\tilde{a}$ defined in (46) to get

$$\frac{1}{\Gamma(-n - i\delta\rho)} \sim -\frac{n!}{\pi}\sin[\pi(n + i\delta\rho)] \sim (-1)^{n+1} n! i\delta\rho, \tag{A3}$$

where in the first approximation we used $\delta\rho \sim 0$ to obtain $\Gamma(1+n+i\delta\rho) \sim \Gamma(1+n)$, and in the second approximation we used $\sin(x+y) = \sin x \cos y + \cos x \sin y$ together with $\sin(i\pi\delta\rho) \sim i\pi\delta\rho$ (valid for small $\delta\rho$).
The relations (A1)–(A3) allow us to go from (47) into (48).

(ii) Finally, we derive the relations needed to make the transition from (49) into (50). Use of $\Gamma(1+x) = x\Gamma(x)$ yields

$$\frac{\Gamma(l+1-i2\varpi)}{\Gamma(-l-i2\varpi)} = i(-1)^{l+1} 2\varpi \prod_{j=1}^{l}(j^2 + 4\varpi^2),$$
$$\frac{\Gamma(-2l-1)}{\Gamma(-l)} = (-1)^{l+1}\frac{l!}{(2l+1)!}. \tag{A4}$$

APPENDIX B: ANALYTICAL RESULTS FOR THE UNBOOSTED CASE

In Secs. II, III, and IV, we have studied the instability of a *massless* scalar field with KK momentum in the boosted Kerr black string geometry. When we *turn off* the boost, the problem is equivalent to the instability of a *massive* scalar field in the Kerr black hole background, as long as we identify the KK momentum with the mass of the scalar field. This last problem was studied originally by Detweiler [18]. To clarify this equivalence, and as a check of our results, in this appendix we show that our analysis yields the results of [18] when we set $\sigma = 0$. In this case we can give the quantitative features of the instability in an approximated analytical form.

When the boost is switched off, the second relation of (39) becomes simply

$$\rho = \frac{M\kappa^2}{\sqrt{\kappa^2 - \omega^2}}. \tag{B1}$$

Use of (45) in (B1) yields $M\kappa^2/\sqrt{\kappa^2-\omega^2} = l + N + 1 + i\delta\rho$. Letting $\omega = \omega_{\rm R} + i\omega_{\rm I}$, one has $\kappa^2 - \omega^2 \sim \kappa^2 - \omega_{\rm R}^2$ since $\omega_{\rm I} \ll \omega_{\rm R}$. Moreover, taking $\delta\rho \ll l + N + 1$ one gets

$$\omega_{\rm R}^2 \approx \kappa^2\left[1 - \left(\frac{\kappa M}{l+n+1}\right)^2\right], \tag{B2}$$

and thus $\omega_{\rm R} \sim \kappa$ since the results are valid in the regime $\kappa M \ll 1$. Moreover, differentiating (B1), $\delta\rho \approx M\kappa^2(\kappa^2-\omega^2)^{-3/2}\omega\delta\omega$, and use of $\omega_{\rm R} \sim \kappa$, $\delta\omega \equiv \omega_{\rm I}$ and (B2) yields

$$\omega_{\rm I} \approx \frac{\delta\rho}{M}\left(\frac{\kappa M}{l+n+1}\right)^3, \tag{B3}$$

with $\delta\rho$ given by (50). Expressions (B2) and (B3) are exactly the relations for the real and imaginary parts of the unstable modes found originally by Detweiler [18], for a massive scalar field with mass κ propagating in the unboosted Kerr background.

[1] F. R. Tangherlini, Nuovo Cimento **77**, 636 (1963).
[2] R. C. Myers and M. J. Perry, Ann. Phys. (N.Y.) **172**, 304 (1986).
[3] R. Emparan and H. S. Reall, Phys. Rev. Lett. **88**, 101101 (2002).
[4] G. T. Horowitz and A. Strominger, Nucl. Phys. **B360**, 197 (1991).
[5] Y. Morisawa and D. Ida, Phys. Rev. D **69**, 124005 (2004)
[6] H. Elvang, Phys. Rev. D **68**, 124016 (2003).
[7] H. Elvang and R. Emparan, J. High Energy Phys. 11 (2003) 035.
[8] R. Emparan, J. High Energy Phys. 03 (2004) 064; H. S. Reall, Phys. Rev. D **68**, 024024 (2003); **70**, 089902(E) (2004).
[9] H. Elvang, R. Emparan, and P. Figueras, J. High Energy Phys. 02 (2005) 031.
[10] T. Mishima and H. Iguchi, Phys. Rev. D **73**, 044030 (2006).
[11] P. Figueras, J. High Energy Phys. 07 (2005) 039.
[12] H. Kodama and A. Ishibashi, Prog. Theor. Phys. **110**, 701 (2003); **110**, 901 (2003).
[13] R. Gregory and R. Laflamme, Phys. Rev. Lett. **70**, 2837 (1993); Nucl. Phys. **B428**, 399 (1994).
[14] R. Emparan and H. S. Reall, Gen. Relativ. Gravit. **34**, 2057 (2002).
[15] J. L. Hovdebo and R. C. Myers, Phys. Rev. D **73**, 084013 (2006).
[16] W. H. Press and S. A. Teukolsky, Nature (London) **238**, 211 (1972).
[17] V. Cardoso, O. J. C. Dias, J. P. S. Lemos, and S. Yoshida, Phys. Rev. D **70**, 044039 (2004); **70**, 049903(E) (2004).
[18] T. Damour, N. Deruelle, and R. Ruffini, Lett. Nuovo Cimento Soc. Ital. Fis. **15**, 257 (1976); S. Detweiler, Phys. Rev. D **22**, 2323 (1980); H. Furuhashi and Y. Nambu, Prog. Theor. Phys. **112**, 983 (2004).
[19] V. Cardoso and O. J. C. Dias, Phys. Rev. D **70**, 084011 (2004).
[20] D. Marolf and B. C. Palmer, Phys. Rev. D **70**, 084045 (2004).
[21] V. Cardoso and J. P. S. Lemos, Phys. Lett. B **621**, 219 (2005).
[22] V. Cardoso and S. Yoshida, J. High Energy Phys. 07 (2005) 009.
[23] R. Emparan and R. C. Myers, J. High Energy Phys. 09 (2003) 025.
[24] J. L. Friedman, Commun. Math. Phys. **63**, 243 (1978).
[25] N. Comins and B. F. Schutz, Proc. R. Soc. A **364**, 211 (1978).
[26] V. Cardoso, O. J. C. Dias, J. L. Hovdebo, and R. C. Myers, Phys. Rev. D **73**, 064031 (2006); V. Jejjala, O. Madden, S. F. Ross, and G. Titchener, Phys. Rev. D **71**, 124030 (2005).
[27] V. Cardoso, O. J. C. Dias, and S. Yoshida, Phys. Rev. D **72**, 024025 (2005).
[28] R. Emparan and H. Reall (unpublished).
[29] R. Emparan and C. Herdeiro (private communication). The Myers-Perry black hole has a Killing tensor and thus the scalar wave equation and Hamilton-Jacobi equations do separate; see [44].
[30] G. T. Horowitz and K. Maeda, Phys. Rev. Lett. **87**, 131301 (2001); B. Kol, J. High Energy Phys. 10 (2005) 049; T. Wiseman, Classical Quantum Gravity **20**, 1137 (2003); M. W. Choptuik, L. Lehner, I. Olabarrieta, R. Petryk, F. Pretorius, and H. Villegas, Phys. Rev. D **68**, 044001 (2003).
[31] E. Sorkin, Phys. Rev. Lett. **93**, 031601 (2004).
[32] R. Emparan, Nucl. Phys. **B490**, 365 (1997); for the physical interpretation of factorization, see K. Hong and E. Teo, Classical Quantum Gravity **20**, 3269 (2003); J. B. Griffiths and J. Podolsky, Int. J. Mod. Phys. D **15**, 335 (2006).
[33] M. Nozawa and K. i. Maeda, Phys. Rev. D **71**, 084028 (2005).
[34] M. Ortaggio, P. Krtous, and J. Podolsky, Phys. Rev. D **71**, 124031 (2005).
[35] V. Pravda and A. Pravdova, Gen. Relativ. Gravit. **37**, 1277 (2005); A. Coley and N. Pelavas, Gen. Relativ. Gravit. **38**, 445 (2006).
[36] H. Elvang, R. Emparan, D. Mateos, and H. S. Reall, Phys. Rev. D **71**, 024033 (2005); J. P. Gauntlett, Fortschr. Phys. **53**, 468 (2005).
[37] Ya. B. Zel'dovich, Pis'ma Zh. Eksp. Teor. Fiz. **14**, 270 (1971) [JETP Lett. **14**, 180 (1971)]; Zh. Eksp. Teor. Fiz. **62**, 2076 (1972) [Sov. Phys. JETP **35**, 1085 (1972)]; C. W. Misner, Phys. Rev. Lett. **28**, 994 (1972); J. Bekenstein, Phys. Rev. D **7**, 949 (1973); W. Unruh, Phys. Rev. D **10**, 3194 (1974).
[38] S. A. Teukolsky, Astrophys. J. **185**, 635 (1973).
[39] S. Ross (private communication).
[40] A. A. Starobinsky, Sov. Phys. JETP **37**, 28 (1973); A. A. Starobinsky and S. M. Churilov, Sov. Phys. JETP **38**, 1 (1973); W. G. Unruh, Phys. Rev. D **14**, 3251 (1976).
[41] M. Abramowitz and A. Stegun, *Handbook of Mathematical Functions* (Dover Publications, New York, 1970).
[42] For a detailed discussion of higher-dimensional spheroidal harmonics see Sec. III of E. Berti, V. Cardoso, and M. Casals, Phys. Rev. D **73**, 024013 (2006); **73**, 109902(E) (2006).
[43] There are two small typos in [22] that do not change the physical results: One is in the last line of (A.7), and the

other is that Fig. 7.b does not have a potential well. I thank V. Cardoso and S. Yoshida for pointing them out.
[44] V. P. Frolov and D. Stojkovic, Phys. Rev. D **67**, 084004 (2003); **68**, 064011 (2003).
[45] S. A. Teukolsky and W. H. Press, Astrophys. J. **193**, 443 (1974).
[46] R. C. Myers, Phys. Rev. D **60**, 046002 (1999).
[47] R. Emparan and R. C. Myers (private communication).
[48] In higher dimensions, there is a richer variety of topologies. For a review see, e.g., H. Elvang, T. Harmark, and N. A. Obers, J. High Energy Phys. 01 (2005) 003; T. Harmark and N. A. Obers, hep-th/0503020.